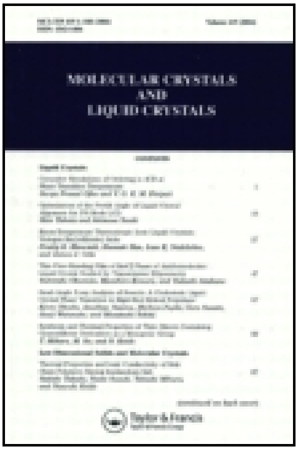

Molecular Crystals and Liquid Crystals
Publication details, including instructions for authors and subscription information:
http://www.tandfonline.com/loi/gmcl20

X-ray and Dielectric Measurements of Smectic A-Hexatic B Transition in Bulk and Confined Geometries

Chethan V. Lobo [a], S. Krishna Prasad [a] & D. S. Shankar Rao [a]

[a] Centre for Liquid Crystal Research, Jalahalli, Bangalore, India

Version of record first published: 31 Aug 2006

To cite this article: Chethan V. Lobo, S. Krishna Prasad & D. S. Shankar Rao (2005): X-ray and Dielectric Measurements of Smectic A-Hexatic B Transition in Bulk and Confined Geometries, Molecular Crystals and Liquid Crystals, 438:1, 151/[1715]-162/[1726]

To link to this article: http://dx.doi.org/10.1080/15421400590955037

Mol. Cryst. Liq. Cryst., Vol. 438, pp. 151/[1715]–162/[1726], 2005
Copyright © Taylor & Francis Inc.
ISSN: 1542-1406 print/1563-5287 online
DOI: 10.1080/15421400590955037

X-ray and Dielectric Measurements of Smectic A-Hexatic B Transition in Bulk and Confined Geometries

Chethan V. Lobo
S. Krishna Prasad
D. S. Shankar Rao
Centre for Liquid Crystal Research, Jalahalli, Bangalore, India

Calorimetric, X-ray and dielectric measurements on a liquid crystal exhibiting a smectic A-Hexatic B (Sm A-Hex B) transition in bulk and upon confinement in Anopore matrix are reported. In the calorimetric experiments the sample in the Anopore matrix shows a much stronger rate-dependent shift in the transition temperature than in the bulk. X-ray studies on both the bulk and the Anopore samples reveal the presence of unusually strong second harmonic reflection arising from the smectic layers in both the Sm A and Hex B phases. From the dielectric measurements it is seen that the director dynamics is marginally influenced by confinement.

Keywords: anopore membrane; confined geometry; dielectric; hexatic B; smectic A; X-ray

INTRODUCTION

The hexatic liquid crystalline phase (Hex B) was first theoretically predicted [1] and then later experimentally observed [2]. This phase has a layered structure, with the molecules oriented along the layer normal direction, and exhibits short-range positional order within the layer just as in the smectic A (Sm A) phase. However, unlike the Sm A phase, the Hex B possesses a bond-orientational order defined as the orientational ordering of the geometric bonds connecting the neighbouring molecules in the plane of the layers. Despite the Sm A-Hex B transition being well studied in the bulk and free-standing geometries [3], the influence of the material being confined to well-defined nano-scale

---

A research grant from the U.S. Office of Naval Research (ONR Grant No. N00014-97-1-0904) is thankfully acknowledged.

Address correspondence to S. Krishna Prasad, Centre for Liquid Crystal Research, Jalahalli, Bangalore 560013, India. E-mail: skprasad1@yahoo.com

pores, had not been studied. Recently [4] we have reported the influence of confinement of the material in Anopore membranes on the Sm A-Hex B transition. Among the various porous substances that can be used for the purpose, the Anopore membranes are attractive as they have highly parallel cylindrical pores with narrow pore size distributions and smoother cavity surface. We would like to emphasize that the studies discussed here should be seen in the light of such work done in systems with transitions involving the nematic (N) [5–9], Sm A [10,11], chiral smectic C (Sm C*) [12–15] and crystal B [16,17] phases.

EXPERIMENTAL

Studies have been carried out on n-butyl 4′-n-hexyloxybiphenyl-4-carboxylate (46OBC for short), having the following phase sequence in bulk [18]

$$\text{Iso } 92.1^\circ\text{C Sm A } 66.8^\circ\text{C Hex B}$$

The Anopore membranes purchased from Whatman, USA have parallel cylindrical pores penetrating the 60 μm thickness normally, with two different nominal pore sizes of 20 and 200 nm (referred to as AN20 and AN200 hereafter). The care and the procedure adapted to fill the sample into the pores of the Anopore membrane is described elsewhere [4]. Calorimetry experiments were done using a Perkin Elmer DSC7, with the scans taken by keeping the outer chamber of the DSC head at a constant temperature of 20°C, a value determined as a trade-off to achieve the best possible signal/noise ratio and not to have any moisture condensation on the chamber. For measurements on a bulk sample, an empty cup was used as a reference; for measurements on Anopore membranes (AN20) an unfilled membrane of approximately the same size was placed in the reference cup.

Details of the image plate setup (Mac Science DIP1030) used for the X-ray experiments are given in an earlier paper [15]. For the bulk sample measurements, the material was contained in a 1 mm Lindemann capillary. For studies on the sample in the membranes (AN200), we used two different configurations. It is known that if untreated membranes are used, the liquid crystalline molecules tend to align along the pore axis. This is the required configuration to study the in-plane correlations and such measurements were carried out with membranes as received. The measurements of the layering and the associated harmonic peaks require the layer normal to be normal to the X-ray beam direction and thus the molecules have to be orthogonal to the membrane pore axis. To obtain such an alignment the membranes were treated with a long chain acid (palmitic acid), a procedure known to result in the molecules aligned in the plane of the membrane [19].

Dielectric measurements were done on the bulk sample using ITO coated plates with a pre-treatment of silane. A combination of this coating and a 2.4 Tesla magnetic field was used to obtain homeotropically aligned mesophases by slowly cooling the sample from the isotropic phase. For the measurements on the Anopore samples, untreated membranes, which as has already been mentioned, induces homeotropic alignment (molecules oriented along the pore axis) were used. The Anopore membrane was sandwiched between two ITO coated glass plates serving as electrodes. A wide-frequency range impedance analyzer (Solatron model 1260) along with a broadband dielectric converter (BDC-N, Novocontrol) and controlled by WinDeta software (Novocontrol) was employed.

RESULTS AND DISCUSSION

DSC Measurements

Figure 1 shows representative DSC scans obtained with the bulk and Anopore samples while heating the sample from the crystalline phase

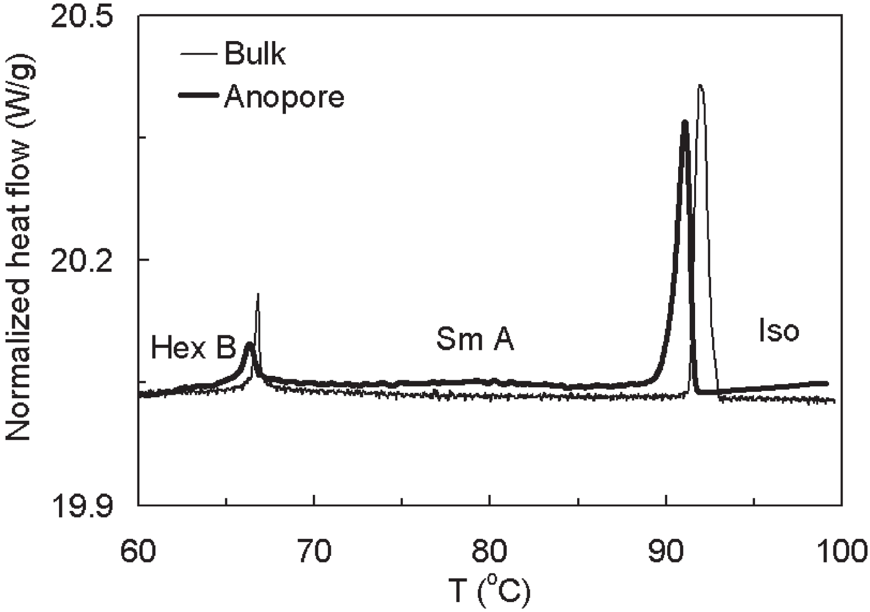

FIGURE 1 Differential scanning calorimetric scan in the heating mode for the bulk and the Anopore sample AN20 obtained with a heating rate of 5°C/min.

at a rate of 5°C/min. It must be mentioned here that for the measurements on the Anopore sample, the quantity of the liquid crystalline material inside the membrane was determined by weighing the membrane before and after filling. For the sake of comparison, the bulk as well as the Anopore data has been normalized with respect to the weight of the liquid crystal. The two peaks seen for the bulk sample correspond to the Hex B-Sm A and Sm A-Iso transitions. This phase sequence and the associated transition temperatures are in very good agreement with the data reported in the literature [18]. The confinement of the sample in the membrane however introduces some differences. Firstly, it broadens both the Iso-Sm A and Sm A-Hex B transitions, although to different degrees: the width for Iso-Sm A increases from 1.5°C to 1.9°C, but the width for Sm A-Hex B gets doubled increasing from 0.8°C to 1.8°C. Secondly, the peak height is essentially the same for the Iso-Sm A transition, whereas for the Sm A-Hex B transition it reduces by a factor of 2. We also observe a small (~1°C) confinement-induced shift in the transition tempera-

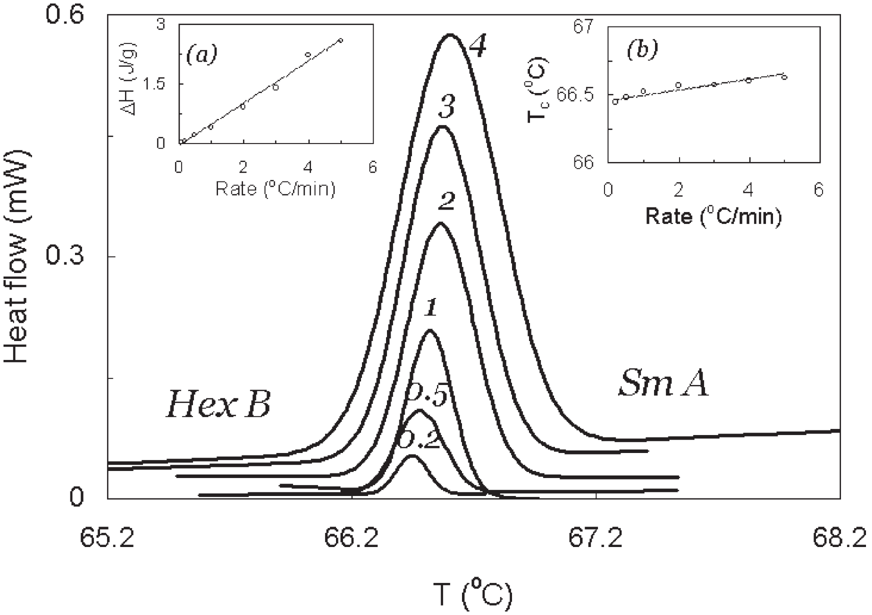

FIGURE 2 Differential scanning calorimetric scans obtained for the bulk sample across the Sm A-Hex B transition for different heating rates (values indicated above each profile). Rate dependence of the Inset (a): transition enthalpy and Inset (b): transition temperature.

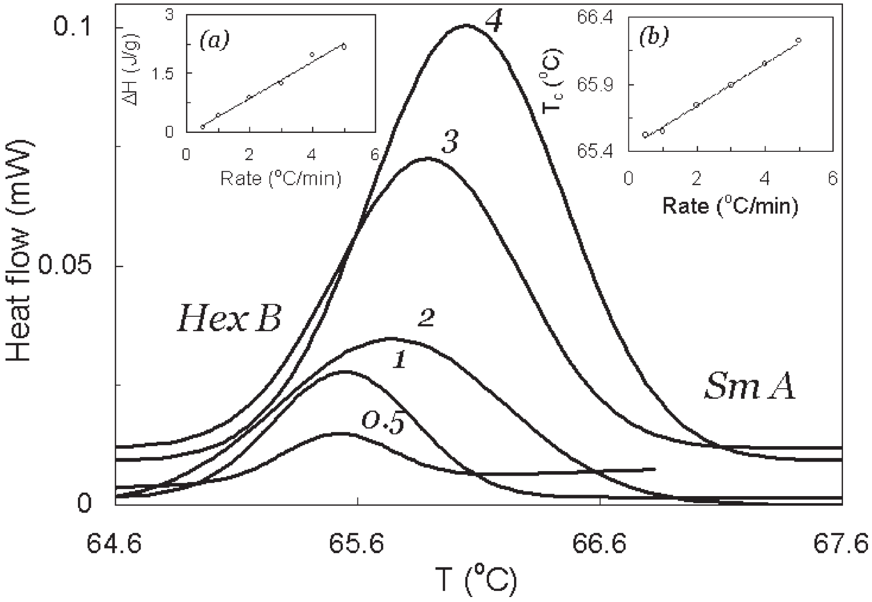

FIGURE 3 Differential scanning calorimetric scans obtained for the Anopore sample AN20 across the Sm A-Hex B transition for different heating rates (values indicated above each profile). Rate dependence of the Inset (a): transition enthalpy and Inset (b): transition temperature.

tures. In the earlier studies [4] we had observed that decreasing the rate of heating of the sample from 5°C to 1°C results in a drastic reduction in the signal level. To confirm this, we performed the measurements in the vicinity of the Sm A-Hex B transition with various heating rates ranging from 0.1°C/min to 5°C/min. Of course, lower rates reduced the signal to noise ratio and therefore we used a profile smoothening algorithm. The scans obtained for the various rates, after this post-processing of the data are shown in Figs. 2 and 3. For the Anopore sample, it was difficult to get data with reliable signal-to-noise ratio for rates less than 0.5°C/min. Notice the drastic decrease in the signal strength as the rate is decreased. Further, the enthalpy values show a monotonic decrease with decreasing rates employed (see inset (a) in Figs. 2 and 3) and the extrapolated value to zero heating rate appears negligibly small, indicating the second order nature of the transition in both the bulk and Anopore samples.

An interesting observation is that with decreasing heating rates, T_c, the temperature corresponding to the peak, (considered as the transition temperature) shows only a marginal decrease in the case of the

(a) Bulk

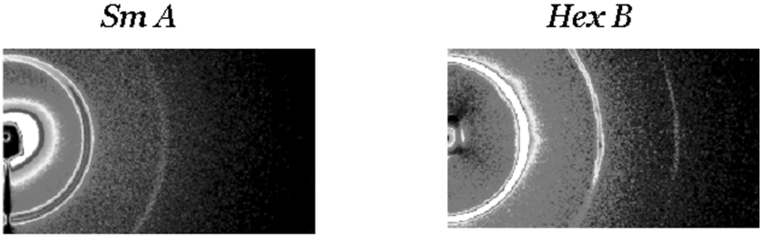

(b) Anopore

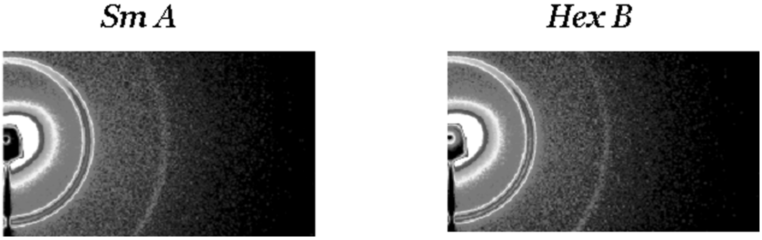

FIGURE 4 Diffraction patterns in the low-angle region of the Hex B phase (right panels) and Sm A phase (left panels) of the (a) bulk and (b) Anopore AN20 samples. The feature to be noted particularly is the presence of higher harmonic reflections.

bulk sample (inset (b) of Fig. 2), but has a substantial change in the case of the Anopore sample (inset (b) of Fig. 3). It may be recalled that transition shifts, peak height suppression and broadening of the transition upon confinement in narrow pores has been well documented in the literature [19].

X-ray Measurements

The diffraction patterns obtained in the low angle region in the Sm A and Hex B phases of the bulk and Anopore samples are shown in Figures 4(a) and 4(b) and the extracted intensity versus diffraction angle (2θ) profiles are shown in Figures 5(a) and 5(b). In the previous paper [4] we had shown that the lowest angle peak is the fundamental and the others are actually the higher harmonic reflections of the fundamental, although with a surprisingly high intensity. It may be recalled that earlier experiments on polar as well as non-polar monomeric compounds had shown that the intensity of the second *(a) Bulk*

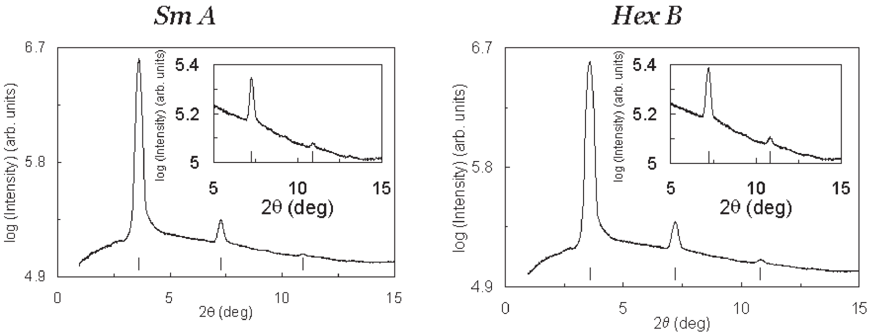

(b) Anopore

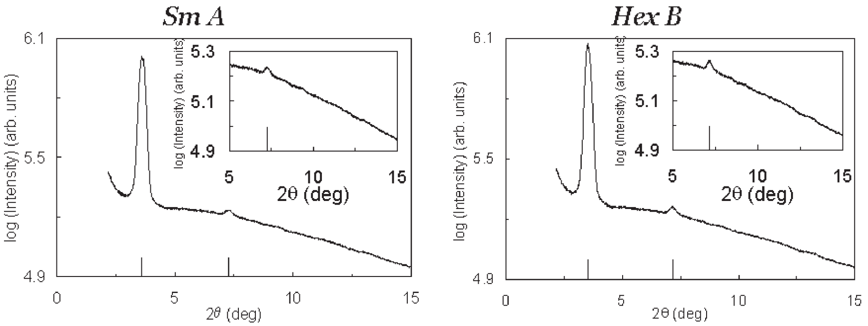

FIGURE 5 One-dimensional intensity vs. 2θ profiles extracted from the diffraction patterns shown in Figure 4.

harmonic reflection is about 10^4 times weaker compared to that for the fundamental [20]. Thus, in the present case the second harmonic is 200 times stronger than commonly observed. Even the third harmonic is an order of magnitude stronger than second harmonic seen for other materials. Generally a second harmonic reflection with sufficient intensity is observed for dimeric materials wherein two aromatic mesogenic units are attached through a flexible aliphatic "spacer" chain. The mutual dislike between the aromatic and the aliphatic parts present in the terminal as well as spacer units perhaps reduces the layer undulation causing the layering to be much well defined than in other compounds. The compound 46OBC is a monomer and therefore the above argument cannot be extended to it. Thus it is surprising to note that it shows such strong higher harmonic reflections. In fact, the second harmonic is seen even when *(a) Bulk*

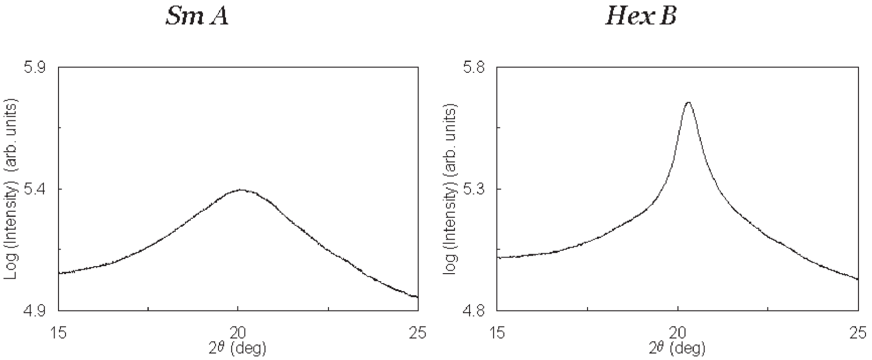

(b) Anopore

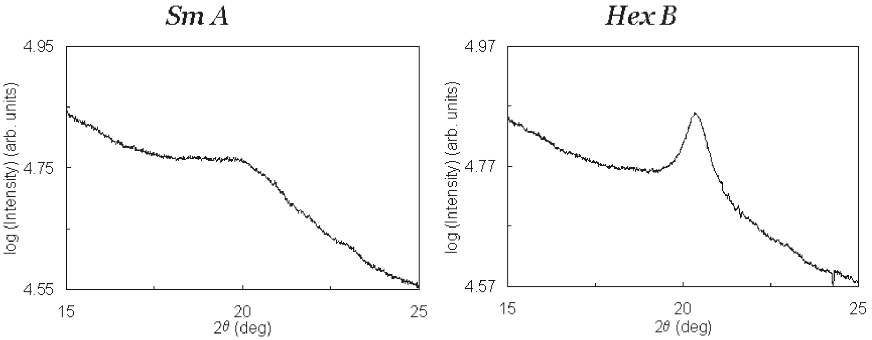

FIGURE 6 One-dimensional intensity vs. 2θ profiles extracted from the diffraction patterns in the wide angle region.

the material is confined in the Anopore membranes although with a slight diminution in the relative strength. (Due to the strong background scattering arising from the Anopore matrix itself, we were not able to separate out the third harmonic reflection from the background noise.)

The in-plane positional ordering within the layer is liquid-like in both the Sm A and Hex B phases, although the extent of correlations should be more for the Hex B phase. The resulting diffraction peak in the wide angle region thus diffuse in both the phases, but relatively sharper in the Hex B phase than the Sm A phase as shown in Figure 6. Fitting the profiles to a Lorentzian form and extracting the parameters of peak position, and the peak width, we had shown that the temperature dependence of these parameters could indeed

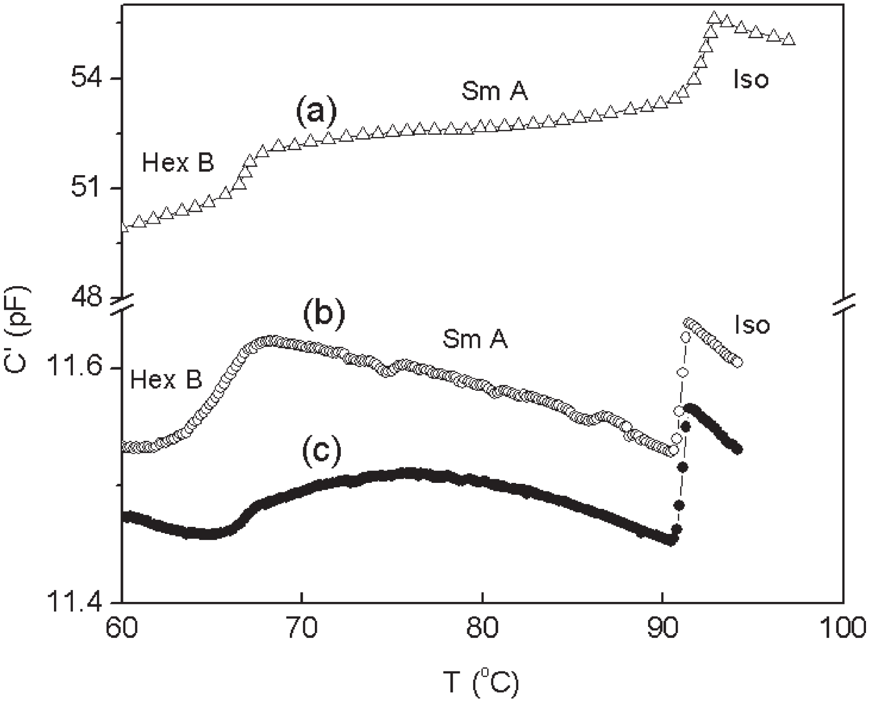

FIGURE 7 Temperature dependence of the sample capacitance in the (a) bulk, (b) Anopore AN200 and (c) Anopore AN20 samples. The transitions are clearly seen in all the samples.

be described by a power-law expression, whose exponent is expected to be the same as the specific heat exponent α. The best fit values of $\alpha = 0.47 \pm 0.01$ obtained for the bulk sample are in close agreement with those reported from X-ray measurements on free-standing films [21] as well as the specific heat studies [22] on the bulk sample. For the Anopore sample, only a marginal increase in the value of α ($= 0.50 \pm 0.01$) was seen suggesting that its critical behaviour is not very different from that for the bulk.

Dielectric Measurements

The temperature variation of the capacitance measured at a fixed frequency for the bulk sample and the Anopore samples AN200 and An20 are shown in Figures 7(a), 7(b) and 7(c) respectively. In the case of the bulk sample, the capacitance value decreases across the Iso-Sm A transition and continues to have a value lower than in the isotropic

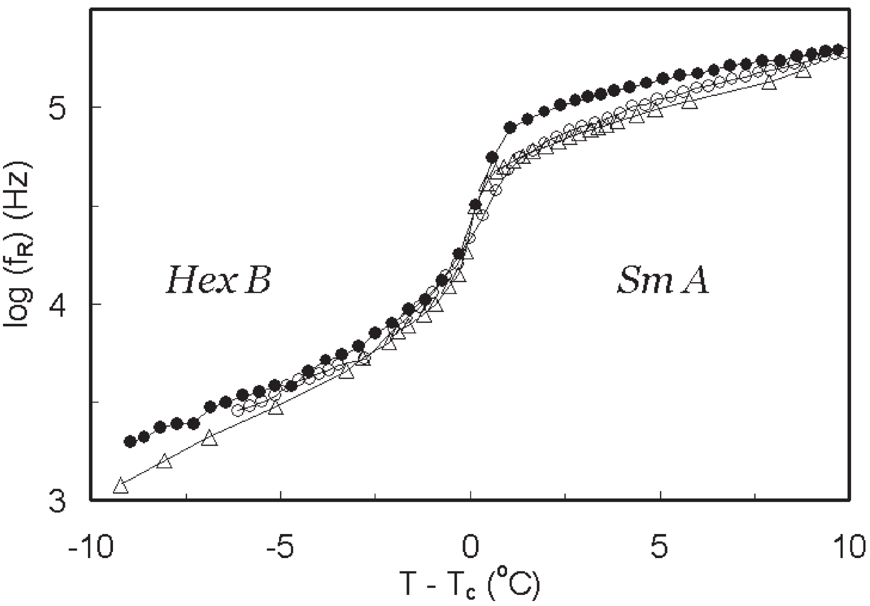

FIGURE 8 Plot showing the thermal variation of the relaxation frequency f_R for the (Δ) bulk, (○) Anopore AN200 and (●) Anopore AN20 samples. Notice that the absolute value of f_R is slightly higher for the Anopore samples.

phase till crystallization, establishing the fact that the material has a negative dielectric anisotropy. The Sm A-Hex B transition is also marked by a clear decrease in the capacitance. For the Anopore samples we see again clear changes across the transitions as well as the feature that values in the mesophases are lower than that in the isotropic phase

The value of the relaxation frequency (f_R) corresponding to the director relaxation mode about the short axes of the molecules, was obtained by fitting the raw C'' ($=C'$x D, where C' is the capacitance and D the loss factor) vs. f data, to the Havriliak–Negami equation [23]. Over the entire range of measurement of both the bulk and Anopore samples, only a single relaxation was seen and the profiles could be very well described by a Debye-relaxation, a feature in confirmation with the second order nature of the Sm A-Hex B transition. The temperature variation of f_R in the bulk and Anopore samples are shown in Figure 8. Unlike in the case of the Sm A-crystal B transition of another material [17], confinement has only a small effect on the absolute value of the relaxation frequency in both the Sm A and Hex B phases. In fact, as the confinement size decreases there is a slight increase in f_R value as compared to that for the bulk sample. Such a behaviour is in agreement with that seen for the N-Iso transition [24], but is at variance with that observed in systems involving a transition to Crystal B phase. For example, across the Sm A-Cr B transition the f_R value decreases by nearly one and two orders of magnitude when the material is confined in 200 nm and 20 nm diameter Anopore membranes respectively [17]. These features are in conformity with the slight reduction in the positional correlation in the Hex B phase of the Anopore sample, as seen by X-ray measurements.

REFERENCES

[1] Birgeneau, R. J. & Litster, J. D. (1978). *J. de Phys. Lett.*, *39*, 399.
[2] Pindak, R., Moncton, D. E., Davey, S. C., & Goodby, J. W. (1981). *Phys. Rev. Lett.*, *46*, 1135.
[3] Brock, J. D., Birgeneau, R. J., Litster, J. D., & Aharony, A. (1989). *Contemporary Physics*, *30*, 321.
[4] Lobo, C. V., Krishna Prasad, S., & Shankar Rao, D. S. (2004). *Phys. Rev. E*, *69*, 051706.
[5] Kuzma, M. & Labes, M. M. (1983). *Mol. Cryst. Liq. Cryst.*, *100*, 103.
[6] Crawford, G. P., Stannarius, R., & Doane, J. W. (1991). *Phys. Rev. A*, *44*, 2558.
[7] Iannacchione, G. S. & Finotello, D. (1992). *Phys. Rev. Lett.*, *69*, 2094.
[8] Dadmun, M. D. & Muthukumar, M. (1993). *J. Chem. Phys.*, *98*, 4850.
[9] Sinha, G. P. & Aliev, F. M. (1998). *Phys. Rev. E*, *58*, 2001.
[10] Iannacchione, G. S., Mang, J. T., Kumar, S., & Finotello, D. (1994). *Phys. Rev. Lett.*, *73*, 2708.
[11] Bellini, T., Clark, N. A., & Schaefer, D. W. (1995). *Phys. Rev. Lett.*, *74*, 2740.
[12] Aliev, F. M. (1996). In: *Liquid Crystals in Complex Geometries*, Crawford, G. P. & Zumer, S. (Eds.), Taylor Francis: London, 345.
[13] Skarabot, M., Kralj, S., Blinc, R., & Musevic, I. (1999). *Liquid Crystals*, *26*, 723.
[14] Rozanski, S. A., Strannarius, R., Krenes, F., & Diele, S. (2001). *Liquid Crystals*, *28*, 1071.
[15] Sandhya, K. L., Krishna Prasad, S., Shankar Rao, D. S., & Bahr, Ch. (2002). *Phys. Rev. E*, *66*, 031710.
[16] Werner, J., Otto, K., Enke, D., Pelzl, G., Janowski, F., & Kresse, H. (2000). *Liquid Crystals*, *27*, 1295.
[17] Sandhya, K. L., Geetha G. Nair, Krishna Prasad, S., & Anjuli Khandelwal. (2001). *Liquid Crystals*, *28*, 1847.
[18] Nagabhushan, C., Geetha G. Nair, Ratna, B. R., Shashidhar, R., & Goodby, J. W. (1988). *Liq. Cryst.*, *3*, 175.
[19] Crawford, G. P. & Zumer, S. (Eds.). (1996). In: *Liquid Crystals in Complex Geometries*, (Eds.), Taylor Francis: London.
[20] Cladis, P. E., Stamatoff, J., Guillon, D., Cross, M. C., Bilash, T., & Finn, P. (1981). In: *Advances in Liquid Crystal Research and Applications*, Bata, L. (Ed.), Pergamon Press: Oxford.
[21] Davey, S. C., Budai, J., Goodby, J. W., Pindak, R., & Moncton, D. E. (1984). *Phys. Rev. Lett.*, *53*, 2129.

[22] Pitchford, T., Nounesis, G., Dumrongrattana, S., Viner, J. M., Huang, C. C., & Goodby, J. W. (1985). *Phys. Rev.* A, *32*.

[23] Havriliak, S. & Negami, S. (1966). *J. Polym. Sci. C*, *14*, 99.

[24] Rozanski, S. A., Strannarius, R., Groothues, H., & Kremer, F. (1996). *Liquid Crystals*, *20*, 59.